Published in final edited form as:

Mol Cancer Ther. 2018 February ; 17(2): 474–483. doi:10.1158/1535-7163.MCT-16-0818.

COX-2/sEH Dual Inhibitor PTUPB Potentiates the Anti-tumor Efficacy of Cisplatin

Fuli Wang[1,2,a], **Hongyong Zhang**[1,a], **Ai-Hong Ma**[3,a], **Weimin Yu**[1,4], **Maike Zimmermann**[1], **Jun Yang**[5], **Sung Hee Hwang**[5], **Daniel Zhu**[1], **Tzu-yin Lin**[1], **Michael Malfatti**[6], **Kenneth W Turteltaub**[6], **Paul T. Henderson**[1], **Susan Airhart**[7], **Bruce D. Hammock**[5], **Jianlin Yuan**[2], **Ralph W. de Vere White**[8,*], and **Chong-Xian Pan**[1,8,9,*]

[1]Department of Internal Medicine, School of Medicine, University of California, Sacramento CA 95817

[2]Department of Urology, Xijing Hospital, The Fourth Military Medical University, Xi`an City, Shanxi Province, China, 710032

[3]Department of Biochemistry and Molecular Medicine, School of Medicine, University of California, Sacramento CA 95817

[4]Department of Urology, Renmin Hospital, Wuhan University, Wuhan, Hubei Province, China 430060

[5]Department of Entomology and Nematology, University of California, Davis, CA 95616

[6]Lawrence Livermore National Laboratory, Livermore, CA

[7]The Jackson Laboratory, Bar Harbor, ME

[8]Department of Urology, School of Medicine and Comprehensive Cancer Center, University of California, Sacramento CA 95817

[9]VA Northern California Health Care System, Rancho Cordova, CA 95655

Abstract

Cisplatin-based therapy is highly toxic, but moderately effective in most cancers. Concurrent inhibition of cyclooxygenase-2 (COX-2) and soluble epoxide hydrolase (sEH) results in anti-tumor activity, and has organ protective effects. The goal of this study was to determine the anti-tumor activity of PTUPB, an orally bioavailable COX-2/sEH dual inhibitor, in combination with cisplatin and gemcitabine (GC) therapy. NSG mice bearing bladder cancer patient-derived xenografts were treated with vehicle, PTUPB, cisplatin, GC or combinations thereof. Mouse experiments were performed with two different PDX models. PTUPB potentiated cisplatin and GC therapy, resulting in significantly reduced tumor growth and prolonged survival. PTUPB plus cisplatin was no more toxic than cisplatin single agent treatment as assessed by body weight, histochemical staining of major organs, blood counts and chemistry. The combination of PTUPB and cisplatin increased apoptosis and decreased phosphorylation in the MAPK/ERK and

[*]To whom correspondence should be addressed: Chong-xian Pan, cxpan@ucdavis.edu, Ralph W. deVere White, rwdeverewhite@ucdavis.edu, 4501 X Street, Room 3016, Sacramento, CA 95817, Tel: (916) 734-3771, Fax: (916) 734-7946.
[a]Fuli Wang, Hongyong Zhang and Ai-Hong Ma contributed equally to this work.

PI3K/AKT/mTOR pathways compared to controls. PTUPB treatment did not alter platinum-DNA adduct levels, which is the most critical step in platinum-induced cell death. The *in vitro* study using the combination index method showed modest synergy between PTUPB and platinum agents only in 5637 cell line among several cell lines examined. However, PTUPB is very active *in vivo* by inhibiting angiogenesis. In conclusion, PTUPB potentiated the anti-tumor activity of cisplatin-based treatment without increasing toxicity *in vivo*, and has potential for further development as a combination chemotherapy partner.

Keywords

bladder cancer; PTUPB; cisplatin; patient-derived xenograft model

Introduction

Cisplatin is the most commonly used chemotherapeutic agent in cancer treatment. However, it is only moderately effective in most cancer types and is highly toxic (1). Cisplatin-based first-line combination therapy is associated with a response rate of approximately 50% for metastatic bladder cancer, and induces complete remission in less than 40% at the neoadjuvant setting for this disease (2). Therefore, there is a great unmet need to develop novel therapies to potentiate efficacy and mitigate the toxicity of cisplatin (3).

One potential strategy to improve cisplatin therapy involves modulation of the arachidonic acid (ARA) pathway, which plays numerous roles in inflammation and tumorigenesis. Eicosanoids are lipid mediators derived from ARA by cyclooxygenases (COXs), lipoxygenases (LOXs) and cytochrome P450s (CYPs). Among them, a COX-2 mediated metabolite, prostaglandin E_2 (PGE_2), is pro-inflammatory and pro-angiogenic (4). COX inhibitors, both nonsteroidal anti-inflammatory drugs (NSAIDs) and COX-2 selective inhibitors (coxibs), have been widely used to treat inflammation and pain. Separately, epoxyeicosatrienoic acids (EETs), derived from the metabolism of ARA by CYP epoxygenases, have potent anti-inflammatory, analgesic, antihypertensive, cardio-protective, and organ-protective properties (5-8). However, EETs are rapidly metabolized to inactive diols by soluble epoxide hydrolase (sEH) (9). sEH inhibitors (sEHIs) such as *trans*-4-(4-(3-adamantan-1-yl-ureido)-cyclohexyloxyl)-benzoic acid (*t*-AUCB) maintain the level of EETs *in vivo*, and are now in development for treatment of various diseases. In preclinical studies as well as in clinical trials, sEHIs have displayed excellent safety profiles (10, 11).

EETs transcriptionally inhibit the expression of COX-2 and thus decrease the production of PGE_2 (12). Interestingly, COX-2 overexpression in tumor or stromal cells leads to tumor angiogenesis (13) and coxibs block the production of angiogenic factors, leading to inhibition of proliferation, migration, and vascular tube formation. However, targeting this single component of the ARA pathway with coxibs has failed in human clinical trials for several cancers (14-16). Furthermore, sEHIs synergize the analgesic and anti-inflammatory effects of coxibs (17, 18), prevent gastrointestinal erosion (19), and alter prostacyclin (PGI_2) and thromboxane A2 (TBX_2) ratios associated with blood clotting (17). Therefore, it is desirable to inhibit both COX-2 and sEH in order to maximize antitumor activity and reduce

toxic effects of selective COX-2 inhibition. This dual COX-2/sEH inhibition strategy also may have the potential to protect normal tissues from cisplatin toxicity.

We recently demonstrated that a combination treatment of celecoxib and the sEHI inhibitor *t*-AUCB has synergistic effects for blocking angiogenesis and tumorigenesis in two mouse models of cancer (20). A compound that concurrently inhibits both COX-2 and sEH called (4-(5-phenyl-3-{3-[3-(4-trifluoromethyl-phenyl)-ureido]-propyl}-pyrazol-1-yl)-benzenesulfonamide; PTUPB) (Figure S1) (21) is more effective at inhibiting primary tumor growth and metastasis compared to inhibitors selective to either pathway, either as single agents or in combination. PTUPB acts, in part, by suppressing tumor angiogenesis via selective inhibition of endothelial cell proliferation, without any obvious cytotoxic effects in mice (20).

Here we report assessment of the interaction of cisplatin or gemcitabine plus cisplatin (GC) with PTUPB. We hypothesize that the combination of PTUPB and cisplatin-based therapy potentiates anti-tumor activity without increasing cisplatin toxicity. We extended our work to include recently developed immunodeficient nod scid gamma (NSG) mice bearing patient-derived xenografts (PDX) of bladder cancer (22), and conducted additional mechanistic studies. We observed that *in vivo* PTUPB potentiated cisplatin efficacy without increasing toxicity. PTUPB also improved *in vivo* response to GC therapy. Platinum-DNA adducts were not modulated by PTUPB exposure, indicating an orthogonal mechanism of action compared to DNA alkylation. However, PTUPB enhances apoptosis and downregulates proliferation signaling, especially when combined with cisplatin.

Materials and Methods

Materials and Supplies

Bladder cancer patient-derived xenograft (PDX) models were provided by The Jackson Laboratory (JAX, Bar Harbor, ME). PDXs were developed through subcutaneous implantation from clinical tumor tissues into immunodeficient NOD. Cg-*Prkdc*^{scid} *Il2rg*^{tm1Wjl}/SzJ (NSG; JAX strain #5557) female mice, followed by serial *in vivo* passaging as previously described (22). All experiments utilized PDX models within the first five passages. Cisplatin was purchased from Fresenius Kabi USA, LLC (Lake Zurich, IL). Gemcitabine was purchased from LC Laboratories (Woburn, MA). [^{14}C]carboplatin was purchased from GE Healthcare (Waukesha, WI) and was prepared as described (23, 24). Celecoxib was a gift from Pfizer. PTUPB and *t*-AUCB were synthesized as previously described (21, 24). The bladder cancer cell lines 5637, J82, T24 and TCCSUP were purchased from American Type Culture Collection (ATCC, Manassas, VA) in 2007. Multiple frozen aliquots were established upon the acquisition and all experimental cells were passaged for fewer than 20 passages after reviving from liquid N2. The cell lines were not tested and authenticated by the authors. Cells were cultured in RPMI-1640 medium supplemented with 10% fetal bovine serum (Gibco, Grand Island, NY) and 1% penicillin-streptomycin (Gibco, Grand Island, NY) and incubated at 37°C in 5% CO_2 incubator.

PDX bladder cancer

NSG PDX studies were performed at the University of California Davis with IACUC approval. Experiments were carried out with 6 to 9 week old female NSG mice bearing bladder cancer PDX models (UC Davis ID# BL0293 or JAX Model # TM00016; UC Davis ID#BL0269 or JAX Model #TM00015). When tumors achieved volumes of 100~200 mm^3, mice were randomized to different treatment groups as follows: vehicle control (PEG 300, 10 mL/kg, oral), PTUPB, cisplatin, t-AUCB, celecoxib, combinations of PTUPB and cisplatin, t-AUCB and cisplatin, celecoxib and cisplatin, gemcitabine and cisplatin (GC), PTUPB and GC. PTUPB (30 mg/kg in PEG 300), celecoxib (30 mg/kg in PEG 300), t-AUCB (3 mg/kg in PEG 300) were administered once per day by oral gavage for up to 30 days. Cisplatin (1 mg/ml) was diluted in 0.9 % saline and administered at a dose of 2 mg/kg (IV, tail vein, once per day) on days 1, 2, 3, 15, 16 and 17. Gemcitabine was dissolved in 0.9 % saline and administered at a dose of 150 mg/kg (IP, weekly) for 4 weeks. Animal weight and tumor size were measured twice per week. The tumor volume was calculated with the following formula: length (mm) × width (mm) × width (mm) × 0.5. The percentage of tumor growth inhibition (TGI) was calculated as follows; $100\% \times (1 - [(V^{treated}_{(final\ day)} - V^{treated}_{(initial\ day)})/(V^{control}_{(final\ day)} - V^{control}_{(initial\ day)})])$, where V is tumor volume.

Blood samples from mice were collected and analyzed for complete blood count (CBC), blood urea nitrogen (BUN), aspartate aminotransferase (AST), creatinine and total bilirubin at the Veterinary Medicine Comparative Pathology Laboratory of University of California Davis. The tumor, heart, liver, spleen, lung and kidney were harvested and the tissue samples were fixed in formalin or frozen at -80°C. Tumor sections were stained with hematoxylin and eosin (H&E) or were used for immunohistochemistry analysis. A board-certified pathologist provided detailed interpretation of tumor histomorphology and scoring of immunohistochemical staining. Some of the tumor sections were lysed and chromatographed using SDS-PAGE followed by transfer onto a PVDF membrane. The membranes were blocked in 5% nonfat dry milk for 1 h at room temperature, and probed with p-AKT(S473), p-ERK(Thr202/Tyr204), total-AKT, total-ERK and rabbit monoclonal anti-GAPDH antibodies (Cell Signaling Technology, Beverly, MA). The membranes were then probed with horseradish peroxidase (HRP) tagged secondary antibodies and epitopes were detected using the ECL Plus Western Blotting Detection Reagent (GE Healthcare, Piscataway, NJ). Cell proliferation, apoptosis and angiogenesis assessed with Ki-67, cleaved caspase-3 and CD31 antibodies (Cell Signaling, Danvers, MA) using an immunohistochemistry kit per the manufacturer's instructions (BioGenex, Fremont, CA).

Accelerator mass spectrometry to determine platinum-DNA adduct formation

The ATCC 5637 bladder cancer cell line and NSG-PDX mice were used to assess the impact of PTUPB on [^{14}C]carboplatin-DNA adduct levels as a surrogate of cisplatin-DNA adducts.

Carboplatin-DNA adduct formation in vitro—For cell culture studies, 60-mm dishes of 5637 cell cultures were either pretreated with 10 μM PTUPB for 5 hr followed by 100 μM [^{14}C]carboplatin (36,000 dpm/mL), or simultaneously dosed with PTUPB and [^{14}C]carboplatin. Four hours after carboplatin was added, the cells were washed with PBS. The 4 hr incubation time was chosen due to the *in vivo* carboplatin half-life (1.3-6 hr) in

patients. Cells were harvested at the 4 hr time point in one group of dishes and another group was washed and further incubated for 20 hr with fresh drug-free medium before cell harvest in order to determine DNA repair. Cell pellets were stored at -80°C until DNA extraction.

Carboplatin-DNA adduct formation in vivo—NSG PDX mice bearing BL0293 tumors were dosed at the volume of 10 μL/g of [^{14}C]carboplatin (37.5 mg/kg, ^{14}C at 50,000 dpm/g) via IV bolus injection. PTUPB (30 mg/kg in PEG 400) was administered via oral gavage 1 hr or 16 hr before carboplatin dosing. Mice were sacrificed and tumor tissues harvested 24 hours after carboplatin dosing. DNA was extracted using a Promega Wizard genomic DNA purification kit according to manufacturer's instructions. Ten micrograms of DNA per sample was submitted to Lawrence Livermore National Laboratory (LLNL) for accelerator mass spectrometry (AMS) analysis using previously reported protocol (25).

Median effect analysis to determine *in vitro* drug-drug interaction

The method published by Chou and Talalay was used to determine the extent and nature (synergism, additivity and antagonism) of PTUPB and cisplatin interaction in cell culture (26, 27). PTUPB was dissolved in dimethyl sulfoxide (DMSO) to a final stock concentration of 10 mM. Cisplatin was dissolved in PBS to a final stock concentration of 10 mM. Cells were seeded at 2,000-3,000 cells and 100 μl of medium per well into 96-well plates (Becton Dickinson, Franklin Lakes, NJ), and incubated overnight. Different concentrations of these two drugs were diluted in culture media and added to each well. The plates were then incubated for an additional 72 hours. The control group was dosed with 0.2% DMSO. Cell viability assays (MTS) were performed according to the manufacturer's protocol (Promega, Madison, WI). The absolute 50% inhibitory concentrations (IC_{50}) were calculated as previously described (28). Dose-response curves were generated with GraphPad Prism 5 software (GraphPad Software Inc., La Jolla, CA). The combination indices (CI) were determined based on the method of Chou et al (26). CI values were calculated with CompuSyn software (http://www.combosyn.com/).

Oxylipin profile analysis

Lipid extraction and analysis was performed as previously reported (20). Briefly, for tumor lipid mediator extraction, ~100 mg of tumor tissues was mixed with an antioxidant solution (0.2 mg/mL butylated hydroxytoluene and 0.2 mg/mL triphenylphosphine in methanol), the surrogate solution, and 400 μL of extract solution (0.1% acetic acid with 0.2 mg/mL butylated hydroxytoluene in methanol), and then homogenized. The resulting homogenates were kept overnight at −80 °C. Next day, the homogenates were centrifuged and supernatants were collected. The pellets were washed with 0.1% butylated hydroxytoluene and 0.1% acetic acid in methanol and the supernatants were collected and combined. LC-MS/MS analysis of the extracts were carried out on an Agilent 1200SL liquid chromatographic system coupled to a 4000 QTRAP MS/MS instrument (AB Sciex) as described (29).

Statistics

Data are presented as mean ± standard error of the mean (SEM) or mean ± standard deviation (SD). Group comparisons were carried out using one-way analysis of variance or Student's *t* test. Survival analysis was performed using the Kaplan-Meier method. A *p* value of less than 0.05 was considered statistically significant.

Results

Co-administration of PTUPB potentiated the anti-tumor activity of cisplatin

We previously showed PTUPB had anti-tumor activity in mouse Lewis lung cancer (LLC) and NDL ($Her2^+$, $Ki67^+$, ER/PR negative) breast carcinoma models (20). Here, we determined whether PTUPB possessed anti-tumor activity in human bladder cancer cell lines and PDXs, and synergized with cisplatin treatment. We used bladder cancer PDX models BL0293 and BL0269. These tumor types, like most bladder cancers in the clinic, are only moderately sensitive (BL0293) or resistant (BL0269) to cisplatin (22). Treatment with single agent PTUPB or cisplatin exhibited moderate anti-tumor activity in mice bearing BL0293 tumors (Figure 1). The time required to reach a 7.5 fold increase in tumor volume was used as a reasonably achievable endpoint to evaluate tumor growth among treatment groups. The vehicle only control had a median time to a 7.5-fold increase in tumor volume of 20.0 days, whereas the median times to this endpoints were 24.4 days ($p = 0.085$) and 35.8 days ($p = 0.0003$) for the PTUPB and cisplatin monotherapy groups, respectively. The median time to a 7.5-fold increase in tumor volume in the cisplatin plus PTUPB combination group was significantly longer (60.9 days) than that of either PTUPB ($p = 0.007$) or cisplatin ($p = 0.02$) single agent treatment groups (Figure 1A). Analysis of overall survival showed that single agent PTUPB did not significantly increase survival time compared to control (39.4 days vs. 31.3 days, $p = 0.201$), whereas single agent cisplatin treatment extended survival to 47.0 days ($p = 0.004$). The survival time could be further significantly increased by co-treatment of mice with PTUPB and cisplatin to 60.9 days, which was longer than that of either the PTUPB ($p = 0.007$) or cisplatin ($p = 0.02$) monotherapy groups (Figure 1B). In PDX model BL0269, which is resistant to cisplatin and gemcitabine monotherapy (Figure 1C), tumor growth was significantly inhibited in the PTUPB plus cisplatin combination group ($p = 0.006$). Furthermore, addition of PTUPB to GC resulted in the best inhibition of tumor growth (Figure 1D). We also performed experiments to examine the efficacy of combination treatments of celecoxib with cisplatin and *t*-AUCB with cisplatin in bladder PDX model BL0269. These experiments were performed in order to assess whether concurrent inhibition of COX-2 and sEH by PTUPB was advantageous compared to the use of inhibitors specific to either pathway. We did not observe any potentiation of cisplatin by celecoxib with respect to inhibiting tumor growth, but we observed moderate additive effect of *t*-AUCB with cisplatin (Figure S2). PTUPB has the best and most statistically significant potentiation of cisplatin efficacy amongst these treatment groups.

Even though PTUPB potentiated the anti-tumor efficacy of cisplatin, we did not observe any significant increase in toxicity. In the BL0293 model, compared to vehicle control, PTUPB monotherapy slightly decreased body weight ($p = 0.086$ at day 23; $p = 0.118$ at day 30) while cisplatin treatment led to significant weight loss ($p<0.001$ at day 23; $p = 0.008$ at day

30). The addition of PTUPB to cisplatin therapy did not further increase weight loss (Figure S3A). We did not observe any significant weight loss in the BL0269 groups, regardless of the treatment (Figures S3B, S3C). We also determined complete blood cell count (CBC) and chemistry panels at days 6 and 20 of treatment (Figure S4). No significant difference in blood panel data was observed among all treatment groups compared to the controls. Histology examination of major organs at day 20 revealed cisplatin and combination treatment induced swollen distal tubule cells in kidneys, and cytoplasmic vacuolization (microvesicular steatosis) in hepatocytes. Although these changes were consistent with cisplatin toxicity, they were modest and could be due to normal variations in tissue morphology. However, no such morphology changes were observed in the control and PTUPB monotherapy groups, suggesting that the changes were caused by cisplatin. No other histological changes were observed in other organs (Figure S5).

Combination treatment of cisplatin and PTUPB induced apoptosis but inhibited proliferation and angiogenesis in bladder cancer PDX

Ki-67 is a nuclear non-histone protein that is preferentially expressed in dividing cells, and is frequently used to assess the proliferation state of tissues. The determination of cleaved caspase 3 is commonly used as an indicator of apoptosis. CD31 is another maker being widely used to evaluate angiogenesis. The combination of cisplatin with PTUPB treatment led to a significant decrease of Ki-67 and CD31 expression and substantial increase of cleaved caspase-3 in stained BL0293 tumor tissues when compared to single treatment with PTUPB or cisplatin (Figure 2 and Figure S6). These data demonstrate that the anti-tumor activity of the combination treatment with PTUPB and cisplatin was, at least in part, due to decreased cell proliferation and angiogenesis with increased apoptosis.

Combination treatment of cisplatin and PTUPB significantly reduced the activity of signaling pathways essential for cell growth

The MAPK/ERK and PI3K/AKT/mTOR signaling pathways are shared by many receptor tyrosine kinases and often essential for tumor growth and survival (Figure 3A). To determine how the different treatments affected these two signaling pathways, tumor tissues were collected at day 3 after treatment started, and at day 17 when tumors started to re-grow in the PTUPB and cisplatin groups or were stabilized as in the combination group. While treatment with either PTUPB alone or cisplatin alone did not significantly diminish levels of either phosphorylated activated ERK (p-ERK) or AKT (p-AKT), the combination treatment of PTUPB and cisplatin substantially decreased levels of both p-ERK and p-AKT at day 3. On Day 17, increased levels of p-ERK and p-AKT were observed in the PTUPB and cisplatin combination group (Figure 3B). These data confirmed that combined therapy suppressed bladder cancer growth, at least in part, through these two pathways, while pathway reactivation was associated with tumor adaptation and re-growth.

PTUPB did not alter platinum-DNA adduct formation

As alkylating agents, platinum-based drugs (including cisplatin and carboplatin) kill cancer cells through formation of covalent drug-DNA adducts. We determined whether PTUPB potentiated the anti-tumor activity of platinum agents via increasing DNA adducts by using [^{14}C]carboplatin-DNA adducts as a surrogate marker that is amenable to AMS analysis.

AMS is ultrasensitive for quantification of ^{14}C in biological sample, and was used to measure carboplatin-DNA adduct formation under physiologically relevant drug concentrations (30). Since cisplatin does not have any carbon atoms in the molecule, it cannot be labeled with ^{14}C. Since both cisplatin and carboplatin form the same therapeutically relevant drug-DNA diadducts and share a similar resistance spectrum (31), we used [^{14}C]carboplatin for this part of the study.

First, we determined the effect of PTUPB on carboplatin-DNA adduct formation in cell culture with the bladder cancer cell line 5637 (32). Cultures of 5637 cells were treated with either carboplatin (100 μM) alone or a combination of carboplatin (100 μM) and PTUPB (10 μM). The 100 μM concentration of carboplatin was used based on its maximum blood concentration in patients after chemotherapy and the treatment duration of 4 hours was chosen to simulate carboplatin plasma half-life of 1.5-6.0 hours in patients. PTUPB exposure did not significantly alter platinum-DNA adduct formation after 4 h (528 ± 41 adducts per 10^8 nt with the carboplatin alone versus 593 ± 282 adducts per 10^8 nt with the combination treatment, $p = 0.713$) (Figure 4A). Similarly, pretreatment of cells with 10 μM PTUPB for 5 hours followed by the addition of carboplatin did not alter the carboplatin induced DNA adduct formation (706 +/- 26 adducts per 10^8 nt with the carboplatin alone versus 606 +/- 66 adducts per 10^8 nt with the PTUPB pretreatment ($p = 0.071$) (Figure 4B). Clearly, PTUPB did not impact drug-target binding and metabolism of carboplatin in cell culture.

We next determined whether PTUPB affected the repair of carboplatin-DNA adducts since increased DNA repair is one of the major mechanisms of cellular resistance to platinum-based cancer therapy. To perform this experiment, 5637 cell cultures were treated with carboplatin alone or with PTUPB plus carboplatin combination for 4 hours followed by removal of both drugs, washing and additional culture with drug-free medium for 20 hours. At 24 hours, the platinum-DNA adduct levels were not significantly different in the two treatment groups, suggesting no difference of DNA repair between two treatments (104.1 +/- 17.7 versus 90.8 +/- 9.1 adducts / 10^8 nt with the carboplatin alone or PTUPB plus carboplatin treatment ($p = 0.312$)). The DNA repair rates were 21.2 +/- 1.3 and 25.1 +/- 8.1 adducts / 10^8 nt per hour for the carboplatin alone and PTUPB plus carboplatin treatment groups (p = 0.648), suggesting no difference of DNA repair between these two treatments.

We also determined whether PTUPB influenced carboplatin-DNA adduct levels *in vivo* (Figure 4C). PTUPB was administered either 16 hours or 1 hour before carboplatin injection and tumors were collected 24 hours after carboplatin treatment. Carboplatin-DNA adduct levels from isolated tumor DNA showed no significant difference between tumors that were treated with carboplatin alone, 16 hours of PTUPB ($p = 0.856$) or 1 hour PTUPB ($p = 0.362$) pre-treatment (1070 ± 317 adducts/10^8 nt, 1019 ± 434 adducts/10^8 nt, and 1334 ± 384 adducts/10^8 nt, respectively). The *in vivo* data are fully consistent with the cell line data, and support PTUPB having a fully orthogonal mechanism of action compared to carboplatin and likely cisplatin.

PTUPB and the platinum drug cisplatin showed modest synergistic drug-drug interaction

Since we showed PTUPB potentiated the anti-tumor effect of cisplatin *in vivo* in bladder PDX models, we wanted to further study the mechanism of the combination effect of these two drugs *in vitro*. To address this question, the combination index *(CI)* method (27) was used to determine the drug-drug interaction of PTUPB and cisplatin. First, we determined the effect of single drug treatment on 5637 bladder cancer cells (Figure 5A). Cultures of 5637 cells were treated with increasing concentrations of PTUPB or cisplatin (0, 0.01, 0.1, 1, 2, 5, 10, 20, 50, 100 μM). The IC_{50} of cisplatin and PTUPB on 5637 cells are 4.5 μM and 90.4 μM, respectively. Next, we determined the combination drug effect of PTUPB and cisplatin (Figure 5B). 5637 cells were treated with different concentrations of cisplatin (0, 0.01 0.1, 0.5, 1, 2, 5, 10, 100 μM) in combination with different concentrations of PTUPB (1, 2, 5, 10 μM). The *CI* values of cisplatin and PTUPB were calculated indicating that PTUPB at concentrations of 1, 2, 5 and 10 μM showed modest synergistic effects in combination with cisplatin at 5 μM. In addition to the 5637 cell line, we also assessed the cytotoxicity of PTUPB and cisplatin in other human bladder cancer cell lines T24, J82, TCCSUP. A modest cisplatin potentiation was only observed in the 5637 cell line but not J82, T24 and TCCSUP cell lines (Figure S7). Low or no direct effects on these cell lines is not surprising since we now know that the mechanism of action for PTUPB is predominantly anti –angiogenesis (20) (Figure 2).

Molecular correlative studies of COX-2/sEH inhibitor PTUPB

To test whether PTUPB targets COX-2/sEH and show that inhibition of COX-2 and sEH pathways is involved in the mode of action of PTUPB *in vivo*, we analyzed oxylipin profiles using LC-tandem MS–based lipidomics (33). PTUPB treatment reduced the levels of COX-dependent prostaglandins PGE_2, PGD_2, TXB_2, 6-keto-$PGF_{1\alpha}$ in BL0269 tumors by ~50% ($p < 0.05$), indicating that PTUPB inhibited the COX-2 pathway *in vivo* (Figure 6A). For the sEH dependent metabolites, PTUPB treatment caused an approximately two-fold increase of 12,13-EpOME, and about a 2-fold decrease on the corresponding diol metabolite 12,13-DiHOME. PTUPB also caused an approximately two-fold increase of 10,11-EpDPE, 15,16-EpODE in BL0269 tumors, whereas it had no effect on the corresponding diol metabolites 10,11-DiHDPE and 15,16-DiHODE (Figure 6B). These results indicate that PTUPB inhibited both the COX-2 and sEH pathways in tumor tissue. The lipid mediators from other pathways were not significantly changed (Table S1). Together, these data support that PTUPB inhibits both COX-2 and sEH, although it may have effects on other cellular targets.

Discussion

As a dual inhibitor of COX-2 and sEH, PTUPB potentiated the anti-tumor activity of cisplatin without increasing the toxicity in mice bearing bladder cancer PDXs. We also performed experiments to examine the efficacy of combination treatments of celecoxib plus cisplatin or *t*-AUCB plus cisplatin in a bladder PDX model. We did not observe any potentiation of cisplatin by celecoxib with respect to inhibiting tumor growth. It was reported by Kurtova et al that blocking tumor expression of PGE_2 with celecoxib modulates tumor repopulation after several cycles and abrogates bladder cancer chemoresistance (34). However, these results are not contradictory with our studies. Kurtova et al used a single

PDX from a GC resistant patient (which was paradoxically quite responsive to GC in the mouse); and a different dosing regimen showing that celecoxib did not have a pronounced effect on GC response in their PDX model until the fourth cycle of GC treatment. Our protocol only had two cycles of GC, and was not designed to assess long-term tumor repopulation by cancer stem cells.

We not only showed that PTUPB enhanced cisplatin and GC efficacy, but also began to define the underlying mechanisms of potentiation. The increased efficacy was not due to increased PTUPB-DNA adduct formation. We gathered evidence that the potentiation is possibly due to *in vivo* factors, such as angiogenesis, and reduced activation of proliferation signaling including the AKT and ERK signaling pathways. Treatment with cisplatin and PTUPB *in vivo* decreased the levels of both p-ERK and p-AKT in tumor tissues, suggesting that these two major signaling pathways were down regulated. We previously reported the evidence of anti-angiogenic properties of PTUPB (20).

PTUPB has the potential for improving platinum-based chemotherapy in the clinic. Even though targeted therapy and immunotherapy have emerged as promising therapeutic modalities, cytotoxic chemotherapy will still be the mainstay in the foreseeable future. For example, targeted and immunotherapies currently benefit only a minority of patients with non-small cell lung and bladder cancers. The response rate of immunotherapy in both cancers is approximately 20 percent or less (35, 36).

In conclusion, the COX2/sEH dual inhibitor PTUPB potentiates cisplatin and GC, possibly synergistically, in bladder cancer PDXs *in vivo* without increasing toxicity. PTUPB and cisplatin treatment increases apoptosis and decreases the activity of the AKT and ERK pathways, but does not increase the formation of platinum-DNA adducts, the most critical step of platinum-induced cell death.

Supplementary Material

Refer to Web version on PubMed Central for supplementary material.

Acknowledgments

We would like to thank Dr. Mingyi Chen for providing pathological diagnosis of PDX mice tissue samples, Tsung-Chieh Shih for technical assistance in IHC staining, Christopher Morisseau, Dipak Panigrhy, and Ted Ognibene for technical support in conducting the experiments, and George Cimino for help during manuscript preparation.

Funding: Work was supported in part by Merit Review (Award # I01 BX001784, C.-X. Pan) from the United States (U.S.) Department of Veterans Affairs Biomedical Laboratory Research and Development Program (The contents do not represent the views of the U.S. Department of Veterans Affairs or the United States Government); NCI Cancer Center Support Grant (PI: de Vere White; Grant #: 2 P30 CA 0933730); The Laney Foundation (PI: de Vere White); American Cancer Society Institutional Research Grant (PI: Lin); NIEHS grant R01 ES002710, NIEHS Superfund Research Program grant P42 ES04699, SBIR Phase II contract HHSN261201200048C (P.T. Henderson) and NIDDK grant R01 DK103616, National Institute of Neurological Disorders and Stroke (NINDS) U54 NS079202.

References

1. Ho GY, Woodward N, Coward JI. Cisplatin versus carboplatin: comparative review of therapeutic management in solid malignancies. Critical reviews in oncology/hematology. 2016; 102:37–46. [PubMed: 27105947]
2. Kamat AM, Hahn NM, Efstathiou JA, Lerner SP, Malmstrom PU, Choi W, et al. Bladder cancer. Lancet. 2016
3. Grivas PD, Day KC, Karatsinides A, Paul A, Shakir N, Owainati I, et al. Evaluation of the antitumor activity of dacomitinib in models of human bladder cancer. Molecular medicine. 2013; 19:367–76. [PubMed: 24166682]
4. Xu L, Stevens J, Hilton MB, Seaman S, Conrads TP, Veenstra TD, et al. COX-2 inhibition potentiates antiangiogenic cancer therapy and prevents metastasis in preclinical models. Science translational medicine. 2014; 6:242ra84.
5. Morisseau C, Hammock BD. Impact of soluble epoxide hydrolase and epoxyeicosanoids on human health. Annual review of pharmacology and toxicology. 2013; 53:37–58.
6. Spector AA, Norris AW. Action of epoxyeicosatrienoic acids on cellular function. American journal of physiology Cell physiology. 2007; 292:C996–1012. [PubMed: 16987999]
7. Inceoglu B, Jinks SL, Ulu A, Hegedus CM, Georgi K, Schmelzer KR, et al. Soluble epoxide hydrolase and epoxyeicosatrienoic acids modulate two distinct analgesic pathways. Proceedings of the National Academy of Sciences of the United States of America. 2008; 105:18901–6. [PubMed: 19028872]
8. Shen HC, Hammock BD. Discovery of inhibitors of soluble epoxide hydrolase: a target with multiple potential therapeutic indications. Journal of medicinal chemistry. 2012; 55:1789–808. [PubMed: 22168898]
9. Spector AA, Fang X, Snyder GD, Weintraub NL. Epoxyeicosatrienoic acids (EETs): metabolism and biochemical function. Progress in lipid research. 2004; 43:55–90. [PubMed: 14636671]
10. Chen D, Whitcomb R, MacIntyre E, Tran V, Do ZN, Sabry J, et al. Pharmacokinetics and pharmacodynamics of AR9281, an inhibitor of soluble epoxide hydrolase, in single- and multiple-dose studies in healthy human subjects. Journal of clinical pharmacology. 2012; 52:319–28. [PubMed: 21422238]
11. Lazaar AL, Yang L, Boardley RL, Goyal NS, Robertson J, Baldwin SJ, et al. Pharmacokinetics, pharmacodynamics and adverse event profile of GSK2256294, a novel soluble epoxide hydrolase inhibitor. British journal of clinical pharmacology. 2016; 81:971–9. [PubMed: 26620151]
12. Schmelzer KR, Kubala L, Newman JW, Kim IH, Eiserich JP, Hammock BD. Soluble epoxide hydrolase is a therapeutic target for acute inflammation. Proceedings of the National Academy of Sciences of the United States of America. 2005; 102:9772–7. [PubMed: 15994227]
13. Ghosh N, Chaki R, Mandal V, Mandal SC. COX-2 as a target for cancer chemotherapy. Pharmacological reports : PR. 2010; 62:233–44. [PubMed: 20508278]
14. Gridelli C, Gallo C, Ceribelli A, Gebbia V, Gamucci T, Ciardiello F, et al. Factorial phase III randomised trial of rofecoxib and prolonged constant infusion of gemcitabine in advanced non-small-cell lung cancer: the GEmcitabine-COxib in NSCLC (GECO) study. The Lancet Oncology. 2007; 8:500–12. [PubMed: 17513173]
15. Groen HJ, Sietsma H, Vincent A, Hochstenbag MM, van Putten JW, van den Berg A, et al. Randomized, placebo-controlled phase III study of docetaxel plus carboplatin with celecoxib and cyclooxygenase-2 expression as a biomarker for patients with advanced non-small-cell lung cancer: the NVALT-4 study. Journal of clinical oncology : official journal of the American Society of Clinical Oncology. 2011; 29:4320–6. [PubMed: 21990410]
16. Pan CX, Loehrer P, Seitz D, Helft P, Juliar B, Ansari R, et al. A phase II trial of irinotecan, 5-fluorouracil and leucovorin combined with celecoxib and glutamine as first-line therapy for advanced colorectal cancer. Oncology. 2005; 69:63–70. [PubMed: 16088234]
17. Schmelzer KR, Inceoglu B, Kubala L, Kim IH, Jinks SL, Eiserich JP, et al. Enhancement of antinociception by coadministration of nonsteroidal anti-inflammatory drugs and soluble epoxide hydrolase inhibitors. Proceedings of the National Academy of Sciences of the United States of America. 2006; 103:13646–51. [PubMed: 16950874]

18. Wagner K, Inceoglu B, Hammock BD. Soluble epoxide hydrolase inhibition, epoxygenated fatty acids and nociception. Prostaglandins & other lipid mediators. 2011; 96:76–83. [PubMed: 21854866]
19. Goswami SK, Wan D, Yang J, Trindade da Silva CA, Morisseau C, Kodani SD, et al. Anti-Ulcer Efficacy of Soluble Epoxide Hydrolase Inhibitor TPPU on Diclofenac-Induced Intestinal Ulcers. The Journal of pharmacology and experimental therapeutics. 2016; 357:529–36. [PubMed: 26989141]
20. Zhang G, Panigrahy D, Hwang SH, Yang J, Mahakian LM, Wettersten HI, et al. Dual inhibition of cyclooxygenase-2 and soluble epoxide hydrolase synergistically suppresses primary tumor growth and metastasis. Proceedings of the National Academy of Sciences of the United States of America. 2014; 111:11127–32. [PubMed: 25024195]
21. Hwang SH, Wagner KM, Morisseau C, Liu JY, Dong H, Wecksler AT, et al. Synthesis and structure-activity relationship studies of urea-containing pyrazoles as dual inhibitors of cyclooxygenase-2 and soluble epoxide hydrolase. Journal of medicinal chemistry. 2011; 54:3037–50. [PubMed: 21434686]
22. Pan CX, Zhang H, Tepper CG, Lin TY, Davis RR, Keck J, et al. Development and Characterization of Bladder Cancer Patient-Derived Xenografts for Molecularly Guided Targeted Therapy. PloS one. 2015; 10:e0134346. [PubMed: 26270481]
23. Zimmermann M, Wang SS, Zhang H, Lin TY, Malfatti M, Haack K, et al. Microdose-Induced Drug-DNA Adducts as Biomarkers of Chemotherapy Resistance in Humans and Mice. Mol Cancer Ther. 2017; 16:376–87. [PubMed: 27903751]
24. Hwang SH, Tsai HJ, Liu JY, Morisseau C, Hammock BD. Orally bioavailable potent soluble epoxide hydrolase inhibitors. Journal of medicinal chemistry. 2007; 50:3825–40. [PubMed: 17616115]
25. Ognibene TJ, Bench G, Vogel JS, Peaslee GF, Murov S. A high-throughput method for the conversion of CO2 obtained from biochemical samples to graphite in septa-sealed vials for quantification of 14C via accelerator mass spectrometry. Analytical chemistry. 2003; 75:2192–6. [PubMed: 12720362]
26. Chou TC. Theoretical basis, experimental design, and computerized simulation of synergism and antagonism in drug combination studies. Pharmacological reviews. 2006; 58:621–81. [PubMed: 16968952]
27. Chou TC. Drug combination studies and their synergy quantification using the Chou-Talalay method. Cancer research. 2010; 70:440–6. [PubMed: 20068163]
28. Sebaugh JL. Guidelines for accurate EC50/IC50 estimation. Pharm Stat. 2011; 10:128–34. [PubMed: 22328315]
29. Liu JY, Yang J, Inceoglu B, Qiu H, Ulu A, Hwang SH, et al. Inhibition of soluble epoxide hydrolase enhances the anti-inflammatory effects of aspirin and 5-lipoxygenase activation protein inhibitor in a murine model. Biochem Pharmacol. 2010; 79:880–7. [PubMed: 19896470]
30. Henderson PT, Li T, He M, Zhang H, Malfatti M, Gandara D, et al. A microdosing approach for characterizing formation and repair of carboplatin-DNA monoadducts and chemoresistance. International journal of cancer. 2011; 129:1425–34. [PubMed: 21128223]
31. Henderson PT, Pan CX. Human microdosing for the prediction of patient response. Bioanalysis. 2010; 2:373–6. [PubMed: 21083245]
32. Wang S, Zhang H, Scharadin TM, Zimmermann M, Hu B, Pan AW, et al. Molecular Dissection of Induced Platinum Resistance through Functional and Gene Expression Analysis in a Cell Culture Model of Bladder Cancer. PloS one. 2016; 11:e0146256. [PubMed: 26799320]
33. Thalji RK, McAtee JJ, Belyanskaya S, Brandt M, Brown GD, Costell MH, et al. Discovery of 1-(1,3,5-triazin-2-yl)piperidine-4-carboxamides as inhibitors of soluble epoxide hydrolase. Bioorg Med Chem Lett. 2013; 23:3584–8. [PubMed: 23664879]
34. Kurtova AV, Xiao J, Mo Q, Pazhanisamy S, Krasnow R, Lerner SP, et al. Blocking PGE2-induced tumour repopulation abrogates bladder cancer chemoresistance. Nature. 2015; 517:209–13. [PubMed: 25470039]

35. Powles T, Eder JP, Fine GD, Braiteh FS, Loriot Y, Cruz C, et al. MPDL3280A (anti-PD-L1) treatment leads to clinical activity in metastatic bladder cancer. Nature. 2014; 515:558–62. [PubMed: 25428503]

36. Borghaei H, Paz-Ares L, Horn L, Spigel DR, Steins M, Ready NE, et al. Nivolumab versus Docetaxel in Advanced Nonsquamous Non-Small-Cell Lung Cancer. The New England journal of medicine. 2015; 373:1627–39. [PubMed: 26412456]

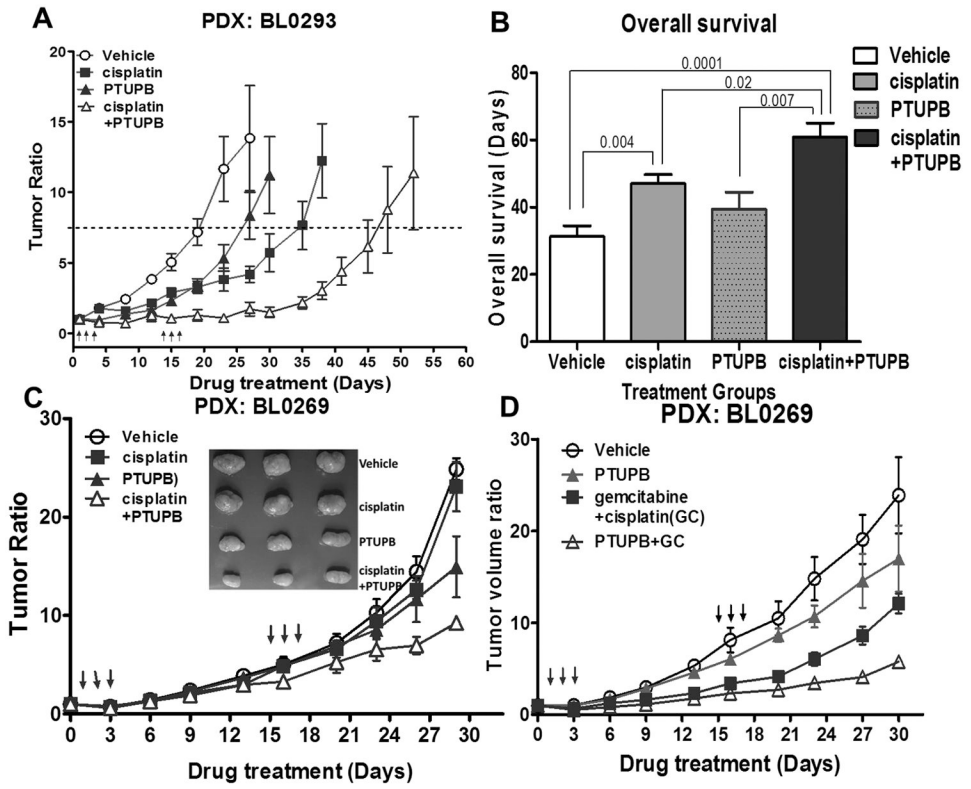

Figure 1. PTUPB potentiates cisplatin anti-tumor activity

A, Tumor growth in NSG-PDX bladder cancer mouse model BL0293. When tumor volume of the tumor reached ~100-200 cm^3, mice were administered by i.v. with PEG 300 control, single agent cisplatin (2 mg/kg, i.v., Day 1, 2, 3, 15, 16, and 17, black arrows), single agent PTUPB (30 mg/kg, orally, once daily for up to 30 days), or cisplatin (2 mg/kg) plus PUTUB (30 mg/kg) in combination. The tumor dimensions were measured every 3~4 days. The tumor volume was calculated using the formula: 0.5 × length × $width^2$ (mm^3). Mice were euthanized when the tumor length reached 20 mm in any direction. The median time of the tumor growth to 7.5× BL (blacked dotted line) was 20 days for the control and 24.4 days in the PTUPB group (p=0.085) and 35.8 days in the cisplatin group (p=0.0003). The median time of the cisplatin and PTUPB combination group was significantly increased to 47.8 days compared to PTUPB (p<0.0001) or cisplatin (p=0.002) monotherapy groups. **B,** Overall survival with statistical analysis. Overall survival of the combination treatment group was 60.9 days, significantly longer than that of either PTUPB (39.4 days, p=0.007) or cisplatin (47 days, p=0.02) monotherapy groups. **C,** Tumor growth in the NSG-PDX bladder cancer mouse model BL0269. Mice were euthanized on day 29 and the tumors were collected. The representative images of the excised tumors are shown. D, Tumor growth in the NSG-PDX bladder cancer mouse model BL0269. When the size of the tumor xenografts reached around 0.1~0.2 cm^3, the NSG mice were treated with PEG 300 control, PTUPB (30 mg/kg, orally, once daily for up to 30 days), cisplatin (2 mg/kg, i.v., Day 1, 2, 3, 15, 16, and 17, black arrows), gemcitabine (150 mg/kg, i.p. weekly for 4 weeks), and cisplatin (2 mg/kg) plus gemcitabine (150 mg/kg) plus PTUPB (30 mg/kg) combination. The tumor sizes were

measured every 3~4 days. The tumor volume was calculated using the formula: 0.5 × length × width^2 (mm^3). N=8-10 mice per group. The results are expressed as mean±SD.

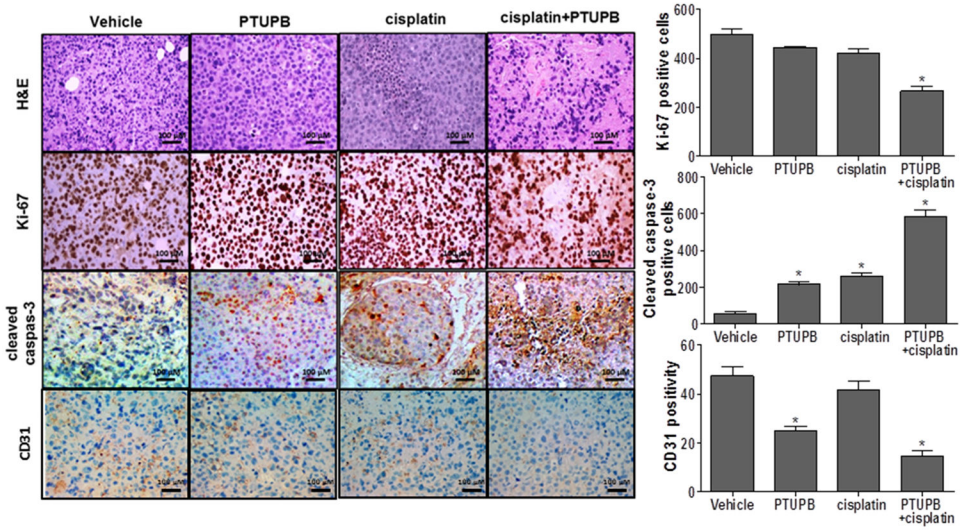

Figure 2. Cisplatin plus PTUPB decreases proliferation and angiogenesis but increases apoptosis as determined by immunohistochemical (IHC) analysis

Formalin-fixed paraffin-embedded PDX BL0293 tumor sections were stained for Hematoxylin and Eosin (H&E), Ki-67, cleaved caspase-3 and CD31. More Ki-67 positive cells were observed in the control group, but significantly decreased in the combination group. Compared with the control group, increasing numbers of cells stained positive for cleaved caspase-3 were observed in the PTUPB, cisplatin, and PTUPB plus cisplatin combination groups. CD31 staining was decreased in PTUPB and combination groups. Quantitative data of Ki67, cleaved caspase-3 and CD31 staining in each group were generated from randomly selected 20 fields and are shown along with the images. *: $p<0.05$.

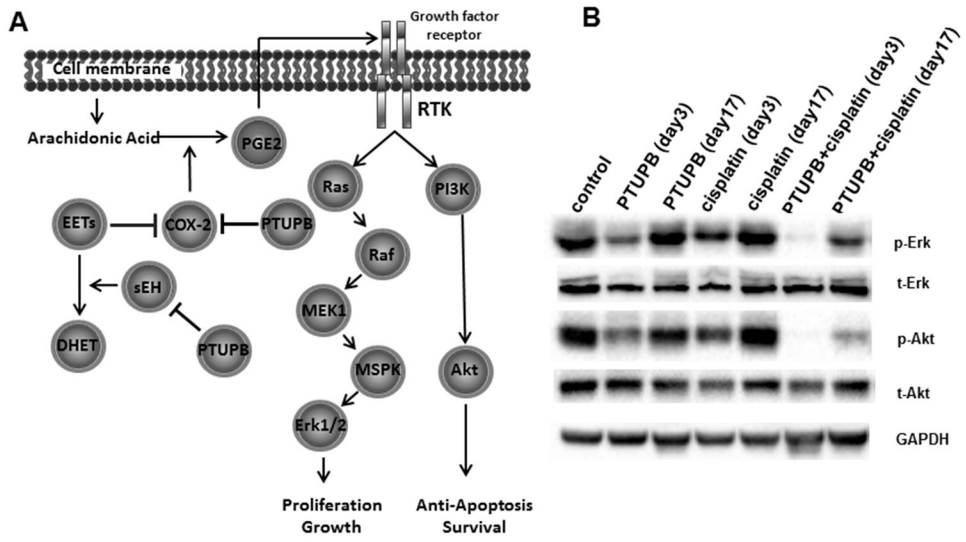

Figure 3. PTUPB combined with cisplatin modulates p-ERK and p-AKT in tumor tissue

A, Illustration of relevant signaling pathways indicating possible roles for sEH and COX-2. **B,** Western blot analysis of protein expression of indicated phospho-proteins, total proteins and loading control GAPDH. Protein was extracted at indicated times from PDX BL0293 tumors treated with cisplatin, PTUPB or cisplatin plus PTUPB combination therapy.

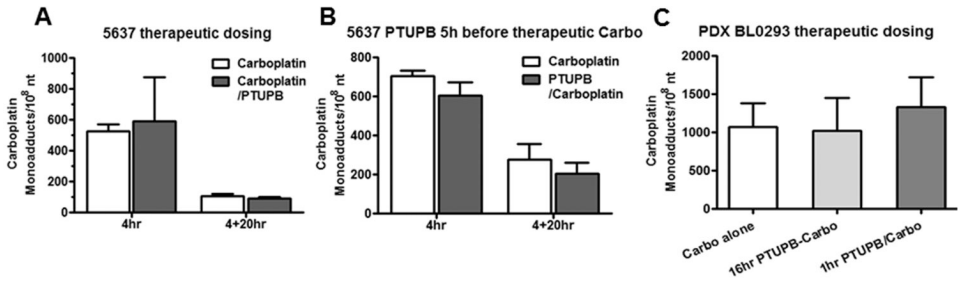

Figure 4. PTUPB does not alter carboplatin-DNA adduct levels

A, Cultures of the ATCC bladder cancer cell line 5637 were incubated with 100 μM [^{14}C]carboplatin in the presence (gray bar) or absence (white bar) of 10 μM PTUPB for 4h or 4h then washed and further incubated 20hr with fresh drug-free culture medium. **B,** 5637 cells were pretreated (grey bar) with 10 μM PTUPB for 5h before cells were exposed to 100 μM [^{14}C]carboplatin for indicated amount of time. **C,** NSG mice carrying BL0293 tumors were treated with 37.5 mg/kg (therapeutic dose) carboplatin (50,000 dpm/g) via IV bolus and tissue was harvested after 24hr. PTUPB (30 mg/kg in PEG400) was administered via oral gavage 16hr (grey bar) or 1hr (black bar) before carboplatin dosing. Sample size for the cell line experiments was N=3, sample size for PDX in experiments was N = 6 (carbo alone) or 3 (in both PTUPB groups). The results are expressed as mean±SD.

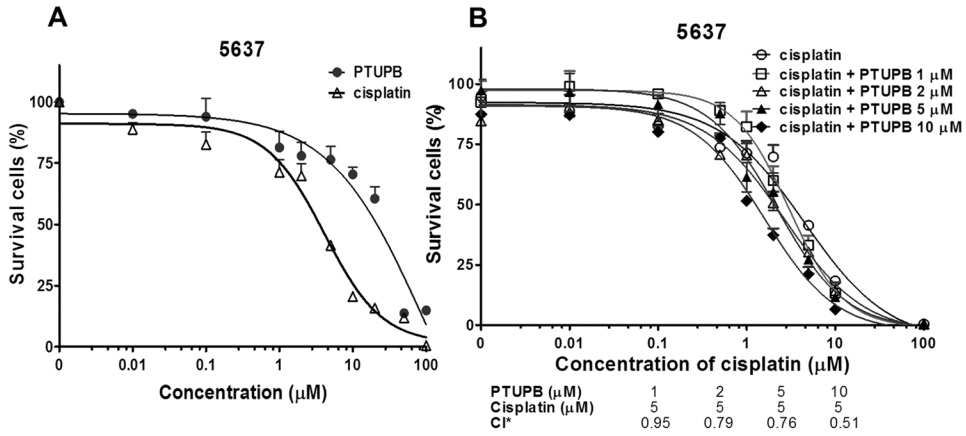

Figure 5. PTUPB increases cisplatin cytotoxicity in the 5637 bladder cancer cell line

Dose-response curves of 5637 cells treated with cisplatin and PTUPB at different concentrations as determined in a 72hr cell viability assay. **A,** Single drug treatment. Cultures of 5637 cells were treated with different concentrations of PTUPB or cisplatin (0, 0.01, 0.1, 1, 2, 5, 10, 20, 50, and 100 μM). **B,** Combination drugs treatment. 5637 cells were treated with different concentrations of cisplatin (0, 0.01 0.1, 0.5, 1, 2, 5, 10, and 100 μM) in combination with different concentrations of PTUPB (1, 2, 5, and 10 μM). Sample size for the cell line experiments was N=3. *CI: Combination Index. The results are expressed as mean±SD.

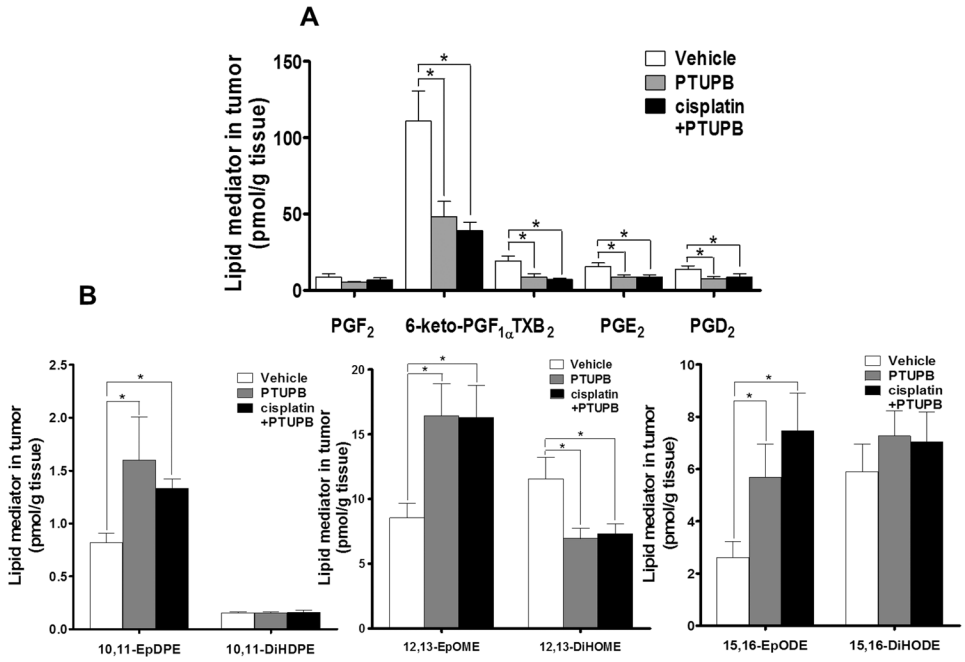

Figure 6. Molecular correlative studies of PTUPB showing inhibition of both COX-2 and sEH pathways in PDX BL0269 tumor tissues

A, PTUPB reduces the levels of prostaglandins PGE_2, PGD_2, TXB_2, 6-keto-$PGF_{1\alpha}$ on COX-2 pathway. **B,** PTUPB increased levels of sEH substrates 10,11-EpDPE, 12,13-EpOME, 15,16-EpODE and decreased levels of sEH product 12,13-DiHOME on sEH pathway. The results are expressed as mean± SD. *P<0.05.